resonance frequency, f_r, of the transducer [16]. It increases away from the resonance frequency, but decreases with increasing pressure [19]. The transducer phase shift varies in a predictable way with frequency [20], and the variation of f_r with pressure has been measured [21]. By determining the phase as a function of pressure at the zero-pressure resonance frequency, f_{r0}, and correcting for the transducer phase shift, the effect of the bond phase shift on the measured pressure derivative of the relevant elastic modulus should amount to less than 0.02 [19]. The relevant combination of elastic moduli is $M = \rho v^2$, where ρ is the density. Expressions for the pressure derivative of M and for the transducer correction are [19]:

$$\frac{\partial M}{\partial P} = -2\frac{M}{\phi}\frac{\partial \phi}{\partial P} + \frac{M}{K_T}(1 - 2K_T\beta_T) + \left(\frac{\partial M}{\partial P}\right)_{\text{corr.}} \quad (3)$$

$$\left(\frac{\partial M}{\partial P}\right)_{\text{corr.}} = \frac{v^2}{L}\frac{Z_t}{f_r}\frac{\partial \ln f_r}{P} \quad (4)$$

where $K_T = \rho(\partial P/\partial \rho)_T$ is the isothermal bulk modulus and $\beta_T = -(\partial \ln L/\partial P)_T$ is the linear compressibility of the sample, and $Z_t = \rho_t v_t$ is the transducer impedance. Expressions for the linear compressibility of tetragonal crystals in any direction, in terms of the elastic compliances or stiffnesses, are given by Nye [14]. Equation (3) contains implicitly the correction for the change in length of the crystal under pressure.

4. Zero-pressure results

The results of the zero-pressure measurements are given in Table 3 in terms of the pseudo-resonance frequency, Δf, of the path, along with the derived elastic wave velocity and corresponding modulus. The X-ray density of 3.178 g/cm^3 [22] was assumed.

The six independent elastic moduli where determined from the eleven mode moduli by requiring a simultaneous least-squares fit to the mode moduli. The resulting best-fit moduli are included in Table 1. The internal consistency of the data is demonstrated by the comparison, in Table 3, of the measured mode moduli with those recalculated from the set of best-fit moduli. The discrepancies of all but modes 10 and 11 are less than 0.3%. Modes 9 and 10 may have been affected by the fact that they are not pure longitudinal and transverse, respectively, so that coupling of modes can occur at reflections. For all modes, an internal consistency within 1% of the mode moduli is assured.

TABLE 3

Measured pseudo-resonance frequencies, velocities and corresponding moduli of various modes in MgF$_2$ at zero pressure. Mode moduli calculated from best-fit c_{ij} (Table 1) are included to show internal consistency

Crystal	Mode	Δf (kHz)	v (km/s)	$M = \rho v^2$ (Mbars)	M (best-fit c_{ij}) (Mbars)	Discrepancy (%)
1	1	370.7	8.005	2.037	2.040	0.2
	2	195.6	4.224	0.567	0.567	0
2	1	371.5	8.023	2.045	2.040	0.3
	2	195.4	4.220	0.566	0.567	0.2
3	3	347.7	6.703	1.428	1.427	0.1
	4	281.1	5.418	0.933	0.935	0.2
	5	218.9	4.220	0.566	0.567	0.2
4	6	377.2	8.146	2.109	2.110	0.1
	7	130.5	2.818	0.252	0.2525	0.2
	8	195.4	4.220	0.566	0.567	0.2
5	9	387.2	7.465	1.771	1.773	0.1
	10	210.9	4.066	0.525	0.527	0.4
	11	253.1	4.879	0.757	0.751	0.9

The six independent moduli are compared with other measurements of MgF_2 in Table 1. The uncertainties given in Table 1 are derived from the deviations from internal consistency (Table 3). Discrepancies between the present results and those of Haussühl [22], Aleksandrov et al. [23] and Jones [24] are somewhat larger: 3% for c_{12} (errors are compounded in deriving this from the measured moduli; see Table 2), and up to 2% for the other moduli. Thus the present data are in quite good agreement with some other recent measurements, although the discrepancies are larger than would be expected from the internal consistency of the data (as is commonly found in ultrasonic measurements). In contrast, the results of Cutler et al. [25] differ from the others by more than 10% in some cases.

5. Pressure derivatives

The measurements of relative phase vs. pressure are illustrated in Fig. 1. Only two of the runs were completed to 7 kbars because of various difficulties. Modes 1, 2, 7 and 8 terminated because the bond deteriorated and the signal was lost. In the initial runs with crystals 1 and 2, the crystals were cracked around the transducer by too rapid decompression (presumably because of differential expansion of the transducer and the sample), in the first case because of a broken seal, and in the second from inexperience. The mode 2 data may be affected by this cracking. The modes 7 and 8 data are not of high quality, be-
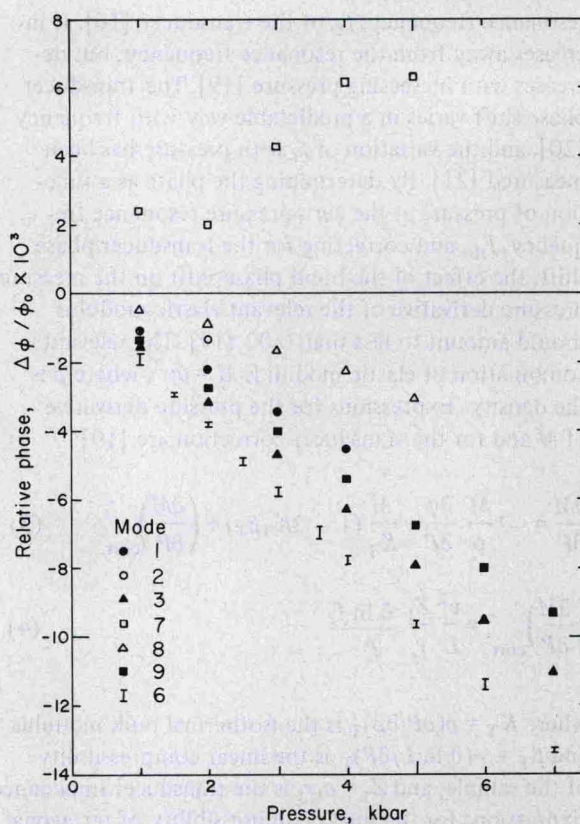

Fig. 1. Measured relative phase increment vs. pressure for indicated modes (Table 2) of MgF_2. Mode 6 data are converted from measurements of frequency shift vs. pressure, using $(\partial \ln \phi/\partial P)_f = -(\partial \ln f/\partial P)_\phi$, without any transducer correction, which is very small in this case. Bars denote results for adjacent constructive and destructive interferences which bracketed the transducer resonance frequency.

TABLE 4

Measure pressure derivatives of phase, and derived pressure derivatives of mode moduli

Mode	$\partial \phi/\partial P$ * (rad/kbar)	$(1/K) - 2\beta$ (Mbar^{-1})	f_r (MHz)	$(\partial M/\partial P)_{corr.}$	$\partial M/\partial P$
1	-0.39 ± 0.01	0.44	20	0.07	5.66 ± 0.15
2	-0.41	0.44	20	-0.03	0.94
3	-0.86 ± 0.01	0.27	10	0.10	5.01 ± 0.06
6	-0.93 ± 0.015 **	0.27	10	0.14	8.59 ± 0.14
7	1.4 ± 0.1	0.27	20	-0.02	-0.68 ± 0.05
8	-0.38 ± 0.05	0.27	20	-0.03	0.79 ± 0.10
9	-0.65 ± 0.01	0.35	10	0.13	5.51 ± 0.08

* Uncertainties estimated from scatter in data (Fig. 1).
** Calculated from measurement of $\partial f/\partial P$.